Cellular Physiology and Biochemistry

Cell Physiol Biochem 2018;48:2374-2388

DOI: 10.1159/000492653

Published online: 16 August, 2018

Accepted: 6 August, 2018

Original Paper

Evidence of Decreased Activity in Intermediate-Conductance Calcium-Activated Potassium Channels During Retinoic Acid–Induced Differentiation in Motor Neuron–Like NSC-34 Cells

Pei-Chun Chen[a,b] Jing-Syuna Ruan[a] Sheng-Nan Wu[a,b]

[a]Department of Physiology, Tainan, [b]Institute of Basic Medical Sciences, College of Medicine, National Cheng Kung University, Tainan City, Taiwan

Key Words

K^+ current • Intermediate-conductance Ca^{2+}-activated K^+ channel • Differentiation • Motor neuron

Abstract

Background/Aims: Intermediate-conductance Ca^{2+}-activated K^+ (IK_{Ca}; $K_{Ca}3.1$ or *KCNN4*) channels affect the behaviors of central neurons including motor neurons. The mechanism through which neuronal differentiation is related to the activity of these channels remains largely unclear. ***Methods:*** By using various molecular biology tools and electrophysiological measurements, we investigated possible changes in the activity of IK_{Ca} channels in a retinoic acid (RA)-induced differentiation process in motor neuron-like NSC-34 cells. ***Results:*** The protein and messenger RNA expression of $K_{Ca}3.1$ substantially diminished as NSC-34 cells were differentiated with low serum (1%) and 1 μM RA. In whole-cell current recordings, the density of delayed-rectifier K^+ currents obtained from differentiated cells was elevated. However, the density of a ramp pulse-elicited K^+ current that was sensitive to blockage by 1-((2-chlorophenyl)(diphenyl)methyl)-1H-pyrazole (TRAM-34)—an inhibitor of IK_{Ca} channels—was significantly higher in undifferentiated NSC-34 cells than in differentiated cells. In undifferentiated cells, the activity of IK_{Ca} channels was readily detected and the probability of channel openings was resistant to stimulation by diazoxide or suppression by verruculogen. Furthermore, this probability was increased by 5,6-dichloro-1-ethyl-1,3-dihydro-2H-benzimidazol-2-one or 9-phenanthrol and reduced by TRAM-34. The channel-opening probability decreased in RA-induced differentiated cells, whereas the single-channel conductance of IK_{Ca} channels did not differ between undifferentiated and differentiated cells. Moreover, the slow component of the mean closed time in these channels was significantly shorter in undifferentiated cells than in differentiated cells; however, the mean open time in the channel remained unchanged as

Sheng-Nan Wu

Department of Physiology, College of Medicine, National Cheng Kung University
No. 1, University Road, Tainan, 70101, (Taiwan)
Tel. 011-886-6-2353535, Fax 011-886-6-2362780, E-Mail snwu@mail.ncku.edu.tw

cells were differentiated. ***Conclusion:*** RA-induced differentiation in neurons could exert a suppressive effect on the activity of IK_{Ca} channels.

Introduction

Intermediate-conductance Ca^{2+}-activated K^+ (IK_{Ca}) channels (also known as $K_{Ca}3.1$, SK4, IKCa1, or *KCNN4*), which are encoded by *KCNN4*, are increasingly being investigated, with a primary focus on various nonexcitable or neoplastic cells with regard to contributory roles in cell behaviors including hormonal secretion, cell migration, cell proliferation, and regulation of Ca^{2+} influx or K^+ efflux [1-6]. Despite being in the same gene family as $K_{Ca}2.x$, $K_{Ca}3.1$ channels share only approximately 45% sequence homology [7]; in particular, these channels exhibit single-channel conductance of 20–60 pS, and their pharmacological profiles are considerably distinguishable from those of large- and small-conductance Ca^{2+}-activated K^+ channels. However, the modulators of functional IK_{Ca} channels have been demonstrated to perturb the functional activities of central neurons including motor neurons [8-13]. More specifically, the activity of these channels increases as voltage-gated Ca^{2+} channels are facilitated by overactivity or neuron recovery (e.g., motor neuron recovery) during spinal cord injuries [8-11]. $K_{Ca}3.1$ channels appear to be strongly linked to a phenotype of hyperactivity disorder, at least in mice [13].

Amyotrophic lateral sclerosis is caused by degeneration of α motor neurons. Because of the low yield of primary motor neurons and the lack of their culture purity, investigations into the molecular responses of motor neurons to neurotoxins and related neuropathological processes require an additional cellular model system. The NSC-34 cell line is a murine neuroblastoma/spinal cord hybrid cell line produced by fusing mouse neuroblastoma cells (N18TG-2, a subclone of mouse C1300 neuroblastoma cells) with motor neuron-enriched embryonic spinal cord cells [14]. This cell line has attracted growing interest as a beneficial model for studying mechanisms underlying neuronal development, differentiation, and oxidative stress [15-18]. N18TG-2 cells differentiated with all-*trans*-retinoic acid (RA) have been utilized as a suitable model to analyze the development of motor neurons, including cholinergic and morphological maturation [19, 20].

RA showed an effect on the morphology and biochemical differentiation of neuronal precursor cells [20]. The present study investigated whether the optimized differentiation of NSC-34 cells by using RA affects the activity of ion channels such as IK_{Ca} (i.e., *KCNN4*-encoded) channels. The results presented in this paper demonstrate that under our experimental conditions, the activity of IK_{Ca} channels was clearly identified in NSC-34 cells, and the functional expression of IK_{Ca} channels observed in differentiated cells became diminished compared with that observed in undifferentiated cells.

Materials and Methods

Drugs and solutions

For this study, 1-((2-chlorophenyl)(diphenyl)methyl)-1H-pyrazole (TRAM-34), 2-chloro-α,α-diphenylbenzeneacetonitrile (TRAM-39), and 5, 6-dichloro-1-ethyl-1, 3-dihydro-2H-benzimidazol-2-one (DCEBIO) were purchased from Tocris Cookson Ltd. (Bristol, UK), 9-phenanthrol, all-*trans*-retinoic acid (RA), and tetrotodoxin were from Sigma-Aldrich (St. Louis, MO), and apamin, iberiotoxin and verruculogen were from Alomone Labs. (Jerusalem, Israel). Chlorotoxin was kindly provided by Professor Dr. Woei-Jer Chuang (Department of Biochemistry, National Cheng Kung University Medical College, Tainan City, Taiwan). Unless stated otherwise, all culture media, fetal bovine (FBS), L-glutamine, trypsin/EDTA, fungizone and penicillin-streptomycin were obtained from Invitrogen (Carlsbad, CA). All other chemicals were commercially and of reagent grade. Deionized water used throughout the experiments was achieved from a Milli-Q water purification system (Millipore, Bedford, MA).

The composition of bath solution (i.e., normal Tyrode's solution) was 136 mM NaCl, 5.4 mM KCl, 1.8 mM $CaCl_2$, 0.53 mM $MgCl_2$, 5.5 mM glucose, and 5.5 mM HEPES-NaOH buffer, pH 7.4. To measure single K^+-channel (e.g., IK_{Ca} channel) activity, pipette solution contained 145 mM KCl, 2 mM $MgCl_2$, and 5 mM HEPES-KOH buffer, pH 7.2. To record whole-cell K^+ currents and avoid contamination of Cl^- currents, the patch pipette was filled with a solution containing 130 mM K-aspartate, 20 mM KCl, 1 mM KH_2PO_4, 1 mM $MgCl_2$, 3 mM Na_2ATP, 0.1 mM Na_2GTP, 0.1 mM EGTA, and 5 mM HEPES-KOH buffer, pH 7.2. To measure IK_{Ca}-channel activity under inside-out configuration, the bath solution was replaced with a high K^+ solution containing 130 mM KCl, 10 mM NaCl, 3 mM $MgCl_2$, 6 mM glucose, and 10 mM HEPES-KOH buffer, pH 7.4. In a separate set of experiments, the pipette was filled with the solution which contained chlorotoxin (1 μM). By use of F-250 fluorescence spectrophotometer and the ratiometric fura-2 measurement, the free Ca^{2+} concentration for high K^+-bathing solution was 208±17 nM (n=7). The free Ca^{2+} concentration was calculated assuming a dissociation constant of 0.1 μM for EGTA and Ca^{2+} (at pH 7.2) (http://maxchelator.stanford.edu/CaEGTA-TS.htm). For example, to provide 0.1 μM Ca^{2+} in the bathing or pipette solution, 0.5 mM $CaCl_2$ and 1 mM EGTA were added. In whole-cell current recordings, to verify the amount of intracellular Ca^{2+} used for elicitation of Ca^{2+}-activated K^+ current, two types of internal pipette solutions with different Ca^{2+}-buffering capacity (i.e., 10 nM and 1 μM Ca^{2+}) were used.

Cell preparation and differentiation

NSC-34 neuronal cells were originally produced by fusion of the motor neuron-enriched, embryonic mouse spinal cords with the mouse neuroblastoma [14, 21]. These cells were kindly provided by Professor Dr. Yuh-Jyh Jong (Department of Pediatrics, Kaohsiung Medical University Hospital, Kaohsiung City, Taiwan). They were routinely grown in Dulbecco's modified Eagle's medium (DMEM) supplemented with 10% (v/v) heat-inactivated fetal bovine serum and 1% penicillin-streptomycin. Cultures were incubated at 37 °C in a humidified environment of 5% CO_2/95% air. The medium was replenished every 2-3 days for removal of non-adhering cells. For long-term storage, the cells were frozen in DMEM containing 10% dimethyl sulfoxide, and kept in liquid nitrogen. Cell viability was evaluated using a MTT cell proliferation assay and an ELISA reader (model 3550; Bio-Rad Laboratories, CA). In attempts to slow cell proliferation and enhance their maturation towards a differentiated state, before confluence, cells were grown in 1:1 mixture of DMEM plus Ham's F12 medium supplemented with low serum (1% FBS) and 1 μM RA [19]. After 6 days of RA treatment, their morphology was changed and became neuron-like cells with interconnected neurites

Assay of cell proliferation

NSC-34 cells (2×10^4) were cultured at 37°C in a 96-well microplate and treated with different concentrations of TRAM-34. After cell exposure to TRAM-34 for 24 hours, 20 μl of methyl tetrazolium (MTT; 3-(4, 5-dimethylthiazol-2-yl)-2, 5-diphenyltetrazolium bromide) solution (5 mg/ml) was added to each well and cells were incubated for another 4 hours. The formazan crystals were dissolved in 150 μl dimethyl sulfoxde and the absorbance of samples was thereafter measured at 490 nm by a microplate reader (model 3550; Bio-Rad Laboratories, CA).

RNA isolation and reverse transcriptase-polymerase chain reaction (RT-PCR)

To detect the expression of $K_{Ca}3.1$ (*KCNN4*) channel messenger RNA in undifferentiated and differentiated NSC-34 neuronal cells, a semi-quantitative RT-PCR assay was performed. Total RNA samples were extracted from cells according to TRIzol reagent protocol (Invitrogen) and reverse transcribed into complementary DNA using Superscript II reverse transcriptase (Invitrogen). The sequences of forward and reverse primers for β-actin were as follows: actin-f: 5'-CGT CTT CCC CTC CAT CG-3'; and actin-r, 5'-CTC GTT AAT GTC ACG CA-3'. The sequences of forward and reverse primers for *KCNN4* were as follows: KCNN4-f, 5'-ACC TTT CAG ACA CAC TTT GG-3'; and KCNN4-r, 5'-TCT CTG CCT TGT TAA ACT CC-3'. The PCR cycling conditions were 30 cycles of 95 °C for 2 min, 95 °C for 30 sec, 60 °C for 30 sec, 72 °C for 30 sec and 72 °C for 10 min. The PCR products were made on 1.5% (w/v) agarose gel containing ethidium bromide and then visualized under ultraviolet trans-illumination. Optical densities of DNA bands were scanned and quantified by AlphaImager 2200 (ProteinSimple; Santa Clara, CA).

Immunofluorescence assay

The cells were initially fixed with 8% paraformaldehyde solution for 10 min and washed 3 times with phosphate-buffered saline (PBS) for 5 minutes each. The permeabilization step was conducted with 1% Triton X-100 which was diluted in PBS and incubated for 2 hours. The cells were then washed 3 times in PBS for 5 minutes each before addition of 1% goat serum for 1 hour. Another wash step with PBS preceded the addition of the primary antibody which was incubated for 2 hours overnight at 4 °C. The primary antibody (the diluted factor for Tuj-1 was 1:500 and for $K_{Ca}3.1$ was 1:250) was diluted in 0.3% Triton X-100 in PBS. Another series of wash steps preceded incubation of secondary antibody (the diluted factor for Tuj-1 and $K_{Ca}3.1$ was 1:200) which was also diluted in 0.3% Triton X-100 in PBS. For controls, the primary antibody was omitted and the secondary antibody was given alone. Cell nuclei were counterstained with 10 μg/ml of Hoechst for 10 min at room temperature. Visualization was made using a Zeiss Axiovert 200M inverted epifluorescence microscope (Jena, Germany) or an Olympus FV1000 confocal laser scanning microscope (Tokyo, Japan).

Electrophysiological measurements

Shortly before the experiments, cells were dissociated with 1% trypsin/EDTA solution and an aliquot of cell suspension was placed on the home-made recording chamber which was positioned on the stage of a CKX-41 inverted fluorescent microscope (Olympus, Tokyo, Japan) coupled to a digital video system (DCR-TRV30; Sony, Japan) with a magnification of up to 1500×. The examined cells were immersed at room temperature (20-25 ºC) in normal Tyrode's solution containing 1.8 mM $CaCl_2$. The electrodes used were pulled from Kimax-51 capillaries (#34500; Kimble Glass, Vineland, NJ) in either a PP-83 puller (Narishige, Tokyo, Japan) or a P-97 Flaming/Brown micropipette puller (Sutter, Novato, CA), and their tips were fire-polished with an MF-83 microforge (Narishige). The pulled electrodes, which had a tip resistance of 3-5 MΩ when filled with different internal solutions described above, was maneuvered using a WR-98 micromanipulator (Narishige). An anti-vibration air table was used to enhance stability during electrophysiological recordings. Patch-clamp recordings were obtained in cell-attached, inside-out, or whole-cell configuration using either an RK-400 (Biol-Logic, Claix, France) or Axopatch 200B (Molecular Devices, Sunnyvale, CA) amplifier [21, 22]. The junctional potentials between the pipette solution and extracellular medium were corrected immediately before seal formation was made.

Data recordings

The signals comprising both voltage and current tracings were monitored on an HM-507 oscilloscope (Hameg, East Meadow, NY) and stored online in a TravelMate-6253 laptop computer (Acer, Taipei City, Taiwan) at 10 kHz through a Digidata 1322A (Molecular Devices) which was equipped with an SCSI card (SlimSCSI 1460; Adaptec, Milpitas, CA) via a PCMCIA slot, and controlled by pCLAMP 9.2 (Molecular devices) during data acquisition. Current signals were low-pass filtered at 1 or 3 kHz. The digitized data were analyzed using either pCLAMP or OriginPro 2016 (OriginLab, Northampton, MA). The pCLAMP-generated voltage-step profiles with either rectangular or ramp pulses were employed to examine the current-voltage (*I-V*) relationships for different types of ionic currents (e.g., delayed-rectifier K+ current $I_{K(DR)}$).

Single-channel analyses

Single IK_{Ca}-channel currents experimentally measured from undifferentiated or differentiated NSC-34 cells were analyzed using pCLAMP 9.2. Single-channel amplitudes were virtually determined by fitting Gaussian distributions to the amplitude histograms of the closed and open states. Channel open probability was defined as $N{\cdot}P_O$, which is estimated using the following expression:

$$N \cdot P_O = \frac{A_1 + 2A_2 + 3A_3 + \ldots\ldots + nA_n}{A_0 + A_1 + A_2 + A_3 + A_4 + \ldots\ldots + A_n}$$

where N is the number of active channels in the patch, A_0 the area under the curve of an all-points histogram corresponding to the closed state, and $A_1 \ldots A_n$ the histogram area that indicates the level of the distinct open state for 1 to n channels in the patch examined. The single-channel conductance was calculated using a linear regression with the mean values of current amplitudes measured at different levels of membrane potentials relative to the bath. Open or closed lifetime distributions of IK_{Ca} channels in

undifferentiated and differentiated cells were fitted with logarithmically scaled bin width.

To determine voltage-dependence of the inhibitory effect of TRAM-34 on the activity of IK_{Ca} channels, the ramp pulses from -90 to 0 mV with a duration of 1 sec were applied. The activation curve was calculated by averaging current traces evoked in response to 20 ramp pulses and subsequently by dividing each point of the mean current by single-channel amplitude for given voltage after the leakage components were corrected. The probabilities of IK_{Ca}-channel openings measured at different membrane potentials were analyzed and then fit using the Woodhull equation taking the form [23]:

$$\frac{P_0}{P} = 1 + \frac{B}{K_0 \cdot \exp\left(\frac{F\delta V}{RT}\right)},$$

or

$$\ln\left(\frac{P_0}{P} - 1\right) = \ln(B) - \ln(K_0) - \left(\frac{F\delta V}{RT}\right)$$

where P_0 is the channel open probability in the absence of TRAM-34 at a given membrane potential, K_0 the equilibrium constant at 0 mV, B the blocker concentration (i.e., TRAM-34), V the membrane potential in mV, F Faraday's constant, R the universal gas constant, F/RT=0.04 mV^{-1}, and T absolute temperature, and δ the fraction of membrane voltage sensed at the binding site (i.e., the effective valence for a monovalent blocker).

Statistical analyses

The linear or non-linear least-squares fitting procedure in this study was appropriately estimated by using either the Solver add-in bundled with Excel™ 2013 (Microsoft, Redmond, WA), or OriginPro 2016 (OriginLab, Northampton, MA). Data are presented as the mean±standard error of mean (SEM), with sample sizes (n) indicating the number of cells in which experimental data were obtained. As we intended to make assertions about the variability of means that could be collected from a random cohort derived from the population concerned, we believe that the standard error shown in this study could be more appropriate than the standard deviation. The paired or unpaired Student's *t*-test, or one-way analysis of variance followed by post-hoc Fisher's least-significance difference test for multiple-group comparisons, were used for the statistical evaluation of differences among means. Statistical analyses were performed using IBM SPSS version 20.0 (IBM Corp., Armonk, NY). Differences were considered significant at $P<0.05$ unless otherwise indicated.

Results

Expression of mRNA for $K_{Ca}3.1$ in undifferentiated and differentiated NSC-34 cells

In the initial set of experiments, we examined the mRNA levels of $K_{Ca}3.1$ (or *KCNN4*) expressed in motor neuron-like NSC-34 cells that had been cultured under conditions set to prompt cell differentiation. Cells were differentiated after being cultured in a 1:1 mixture of DMEM plus Ham's F12 medium

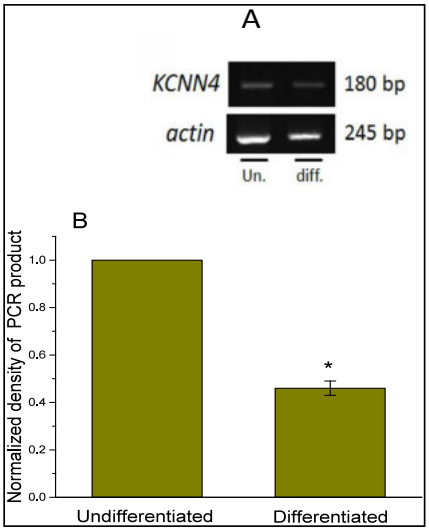

Fig. 1. Expression level of $K_{Ca}3.1$ mRNA isolated from normal (i.e., undifferentiated [Un.]) and differentiated (Diff.) NSC-34 cells. Total RNA was isolated and RT-PCR analysis was performed. In (A), amplified RT-PCR products were obtained with the band of $K_{Ca}3.1$ (180 bp) and β-actin (actin; 245 bp). The PCR replicates were 35 cycles. The fold difference in the density of bands obtained between undifferentiated (Un.) and differentiated (Diff.) cells was approximately two-fold. (B) Bar graph summarizing the quantification of $K_{Ca}3.1$ mRNA that was normalized to the β-actin signal in undifferentiated and differentiated cells. Data are expressed as the mean ± SEM of measurements in three different cultures. *Significantly different from the data of undifferentiated cells ($P<0.05$).

supplemented with 1% serum and 1 μM RA. Consistent with previous studies [19], our RT-PCR results demonstrated that the mRNA of $K_{Ca}3.1$ was clearly detected in undifferentiated and differentiated cells. In addition, under our experimental conditions, the extent of mRNA expression of $K_{Ca}3.1$ in undifferentiated cells was considerably higher than that in differentiated cells (Fig. 1).

Differences in the immunoreactivity of Hoescht, Tuj-1, and $K_{Ca}3.1$ staining between undifferentiated and differentiated NSC-34 cells

Undifferentiated and differentiated NSC-34 cells were further examined using an immunofluorescence assay. Nuclear immunolabeling and neuronal differentiation are indicated by the staining of Hoechst and Tuj-1, respectively. The immunoreactivity of Hoechst staining decreased, whereas that of Tuj-1 staining became strongly demarcated in differentiated NSC-34 cells (Fig. 2b) as compared to undifferentiated NSC-34 cells (Fig. 2a). In addition, the morphology of differentiated cells was markedly altered from that of undifferentiated cells. The results suggested that successful neuronal differentiation had occurred under our experimental conditions. As the image was merged (the combination of Hoechst, Tuj-1, and $K_{Ca}3.1$ staining), punctate immunolabeling of $K_{Ca}3.1$ located at the periphery of each undifferentiated cell was observed. Moreover, the immunoreactivity of $K_{Ca}3.1$ decreased in differentiated NSC-34 cells. Similar results were obtained from four independent experiments.

Comparison of $I_{K(DR)}$ densities between undifferentiated and differentiated NSC-34 cells

The inherent biophysical properties of $I_{K(DR)}$ in both differentiated and undifferentiated NSC-34 cells were further examined. In these experiments, NSC-34 cells were bathed in Ca^{2+}-free Tyrode's solution containing 1 μM tetrodotoxin and 0.5 mM $CdCl_2$. As detailed in Materials and Methods, a recording pipette was filled with a K^+-containing solution. Each examined cell was depolarized from −50 mV to a series of voltages ranging from −50 to 30 mV in 10-mV increments. As illustrated in Fig. 3A and B, after cells had been differentiated using RA, the $I_{K(DR)}$ density in response to membrane depolarization was higher in differentiated NSC-34 cells than in undifferentiated ones. The density versus membrane potential relationship

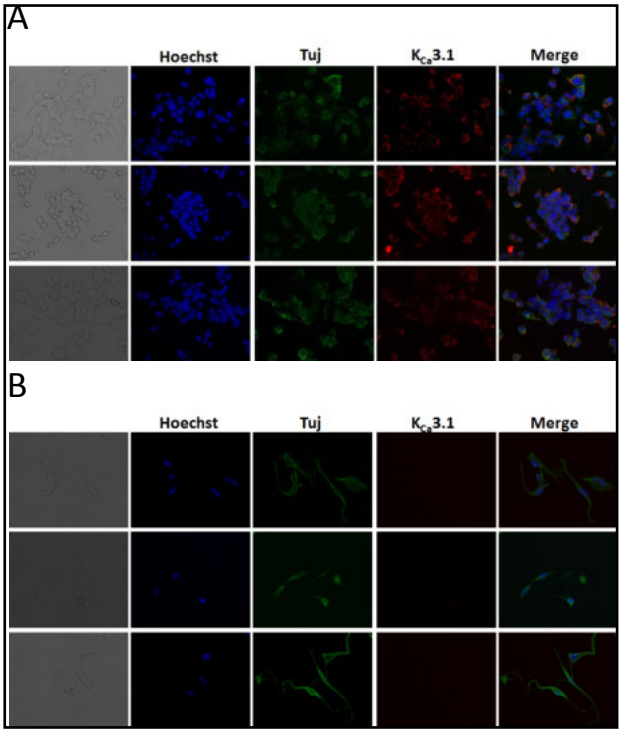

Fig. 2. Immunofluorescence staining of Hoechst, Tuj-1, and $K_{Ca}3.1$ in undifferentiated (A) and differentiated (B) NSC-34 cells. The blue, green, and red colors shown in the images represent the staining of Hoechst (i.e., nuclear immunoreactivity), Tuj-1 (i.e., immunoreactivity for neuronal differentiation), and $K_{Ca}3.1$, respectively. The immunoreactivity for $K_{Ca}3.1$ was clearly decreased in differentiated NSC-34 cells compared with that in undifferentiated cells; however, the immunofluorescent intensity of Tuj-1 staining was higher in differentiated cells. All images were captured under a confocal microscope at 400× magnification.

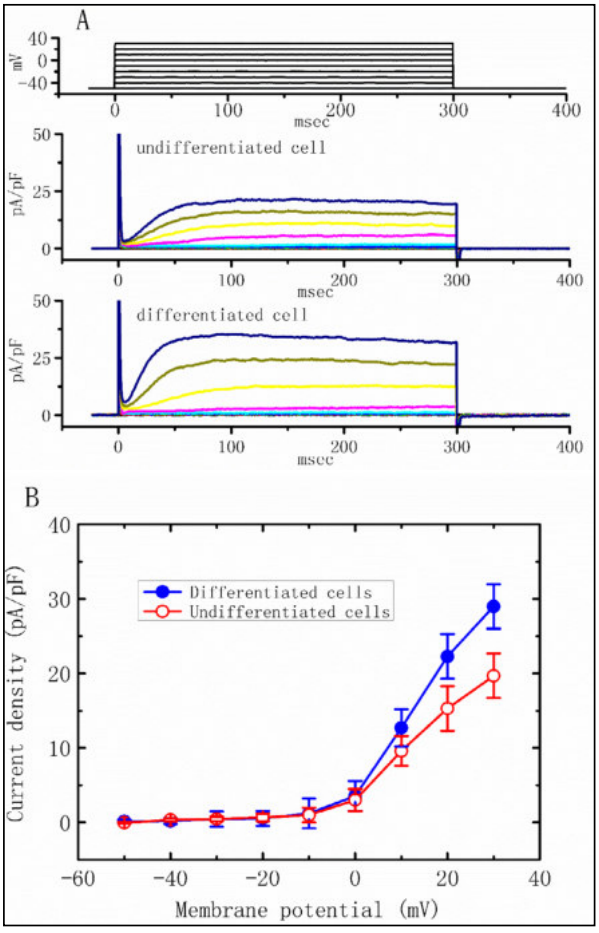

Fig. 3. Electrical properties of $I_{K(DR)}$ measured in undifferentiated and differentiated NSC-34 cells. To induce differentiation, cells were maintained in a culture medium with 1% serum and 1 μM RA. In these experiments, cells were bathed in Ca^{2+}-free Tyrode's solution containing 1 μM tetrodotoxin and 0.5 mM $CdCl_2$, and the recording pipette was filled with a K^+-containing solution. (A) Superimposed $I_{K(DR)}$ traces in undifferentiated (upper) and differentiated (lower) NSC-34 cells. Each examined cell was held at −50 mV, and a series of voltage pulses from −50 to 30 mV in 10-mV increments were applied. The uppermost part indicates the voltage protocol used. (B) Current density versus membrane potential relationships of $I_{K(DR)}$ in undifferentiated (○) and differentiated (●) NSC-34 cells (mean ± SEM; n = 7–10). Notably a significant increase in the density of $I_{K(DR)}$ was observed in differentiated NSC-34 cells.

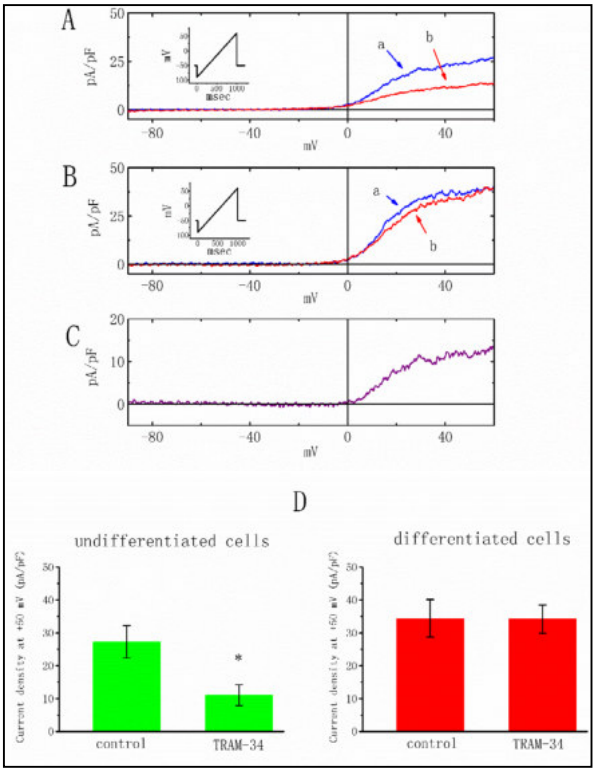

Fig. 4. Inhibitory effect of TRAM-34 on I_K elicited by a long-lasting ramp pulse. In these experiments, cells were bathed in normal Tyrode's solution containing 1.8 mM $CaCl_2$, and the recording pipette was filled with A K^+-containing solution. The examined cell was held at −50 mV, and the ramp pulse was increased from −90 to 50 mV within 1 s. (A) and (B) represent current traces obtained from undifferentiated and differentiated NSC-34 cells, respectively, and "a" and "b" in (A) and (B) indicate the absence and presence of 1 μM TRAM-34 respectively. The inset of each panel indicates the applied voltage protocol. (C) The TRAM-34-sensitive current in undifferentiated NSC-34 cells. The current density (b) obtained after addition of 1 μM TRAM-34 was subtracted from that in the control (a) to yield the TRAM-34-sensitive current (i.e., a-b). (D) Bar graphs showing the effect of TRAM-34 (1 μM) on current density measured at 50 mV in undifferentiated (left) and differentiated cells (mean ± SEM; n = 8–11 for each bar). *Significantly different from control (P<0.05).

of $I_{K(DR)}$ with or without cell differentiation is shown in Fig. 3B. For example, as cells were depolarized from −50 to 30 mV, $I_{K(DR)}$ density in undifferentiated cells was 19.7 ± 2.8 pA/pF (n = 9), which was significantly lower than the corresponding value in differentiated cells (29.1 ± 2.9 pA/pF, n = 9) ($P < 0.05$). However, whole-cell capacitance in undifferentiated NSC-34 cells (32.3 ± 1.9 pF, n = 11) did not differ significantly from that in RA-differentiated cells (32.6 ± 2.1 pF, n = 11) ($P > 0.05$).

Inhibitory effect of TRAM-34 on K^+ current in response to a long-lasting ramp pulse measured in undifferentiated and differentiated NSC-34 cells

The mRNA and protein expression of $K_{Ca}3.1$ became diminished as NSC-34 cells were differentiated using RA. We investigated whether TRAM-34, an inhibitor of IK_{Ca} channels, exerts any differential effects on the K^+ current (I_K) when elicited by a long-lasting ramp pulse. In this set of experiments, NSC-34 cells were bathed in normal Tyrode's solution containing 1.8 mM $CaCl_2$, and the ramp pulse was increased from −90 to 50 mV within 1 s to evoke I_K, in which $I_{K(DR)}$ and various components of Ca^{2+}-activated I_K may be included. The addition of TRAM-34 (1 μM) significantly suppressed the I_K density in undifferentiated NSC-34 cells. The magnitude of TRAM-34-induced suppression (i.e., TRAM-34-sensitive component) was significantly higher in undifferentiated cells than in differentiated cells (Fig. 4); for example, at 50 mV, in undifferentiated cells, the addition of TRAM-34 (1 μM) suppressed I_K by 58.8% ± 3.1% (n = 8), whereas in differentiated cells, TRAM-34 reduced the current by only 0.6% ± 0.1% (n = 8) ($P < 0.01$). However, the addition of neither iberiotoxin (200 nM) nor apamin (200 nM) could suppress the I_K density elicited by a long-lasting ramp pulse. For example, at 50 mV, the I_K density with and without iberiotoxin (200 nM) did not differ significantly (28.3 ± 9 pA/pF [control] vs. 28.2 ± 9 pA/pF [iberiotoxin], n = 8, $P > 0.05$). Iberiotoxin and apamin are known inhibitors of large- and small-conductance Ca^{2+}-activated K^+ channels, respectively. In addition, cell viability on day 2 of culture for undifferentiated cells did not differ significantly between the absence and presence of 1 μM TRAM-34 (87% ± 2% [control] vs. 86% ± 3% [TRAM-34], n = 5, $P > 0.05$).

Activity of IK_{Ca} channels in undifferentiated NSC-34 cells

The cell-attached configuration of the patch-clamp technique was used to investigate the biophysical and pharmacological properties of IK_{Ca} channels in undifferentiated NSC-34 cells. In this series of experiments, the examined cells were bathed in normal Tyrode's solution containing 1.8 mM $CaCl_2$. As shown in Fig. 5A, the activity of IK_{Ca} channels in undifferentiated NSC-34 cells, which occurred in rapid open–close transitions, was clearly detected when the membrane was maintained at −20 mV. Based on an amplitude histogram (Fig. 5B), the single-channel amplitude did not differ between the absence and presence of 1 μM TRAM-34. Moreover, the addition of DCEBIO (10 μM) or 9-phenanthrol (3 μM) significantly increased the probability of channel openings, whereas TRAM-34 (1 μM) was effective in suppressing the activity of IK_{Ca} channels (Fig. 5C). Similarly, TRAM-39 (1 μM)—another inhibitor of IK_{Ca} channels—was effective in suppressing IK_{Ca} channels in undifferentiated NSC-34 cells. DCEBIO and 9-phenanthrol are effective in stimulating IK_{Ca} channels [23-25]. By contrast, when undifferentiated cells were exposed to diazoxide (10 μM), an activator of the ATP-sensitive I_K, or verruculogen (1 μM), an inhibitor of the large-conductance Ca^{2+}-activated K^+ channel, the probability of IK_{Ca}-channel openings in NSC-34 cells did not shift significantly. When the pipette solution was included with 1 μM chlorotoxin—a blocker of Cl^- channels—IK_{Ca} channels remained active and were sensitive to stimulation by DCEBIO or 9-phenanthrol and suppression by TRAM-34 (data not shown). As shown in Fig. 5D, in differentiated NSC-34 cells, the presence of DCEBIO (10 μM) or 9-phenanthrol (3 μM) increased the activity of these channels to a similar extent (i.e., approximately two-fold). When differentiated NSC-34 cells were exposed to 10 μM DCEBIO and 3 μM 9-phenanthrol, the probability of IK_{Ca}-channel openings significantly increased to 0.0081 ± 0.0018 (n = 7, $P < 0.05$) and 0.008 ± 0.0016 (n = 7, $P < 0.05$), respectively, from the control level of 0.0042 ± 0.00009 (n = 7).

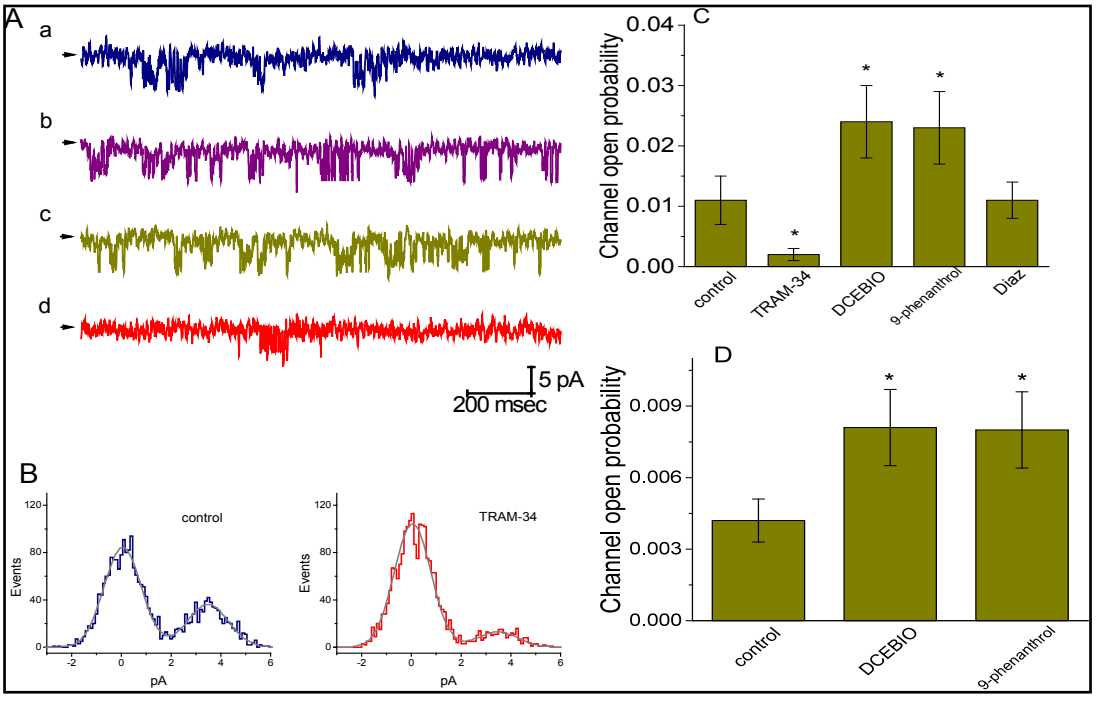

Fig. 5. Electrical and pharmacological properties of IK_{Ca} channels in undifferentiated and differentiated NSC-34 cells. In this set of experiments, cells were bathed in normal Tyrode's solution, cell-attached current recordings were taken, and the examined cell was held at −20 mV relative to the bath. (A) Representative IK_{Ca} channels obtained in the control (i.e., undifferentiated cells; a) and during cell exposure to 10 μM DCEBIO (b), 3 μM 9-phenanthrol (c), or 1 μM TRAM-34 (d). The downward deflection and arrowhead in each trace indicate the opening event of the channel and the zero current level, respectively. (B) Amplitude histogram of IK_{Ca} channels in the absence (left) and presence (right) of 1 μM TRAM-34. (C) Bar graph summarizing the effects of DCEBIO (10 μM), 9-phenanthrol (3 μM), TRAM-34 (1 μM), and diazoxide (10 μM) on the probability of IK_{Ca}-channel openings in undifferentiated NSC-34 cells (mean ± SEM; n = 9–11 for each bar). *Significantly different from control (i.e., in the absence of any agent) (P<0.05). (D) Bar graph summarizing the effects of DCEBIO (10 μM) and 9-phenanthrol (3 μM) on IK_{Ca}-channel activity in differentiated cells (mean ± SEM; n = 8 for each bar). *Significantly different from control (P<0.05).

Comparison of IK_{Ca}-channel activity in undifferentiated and differentiated NSC-34 cells

In these experiments, NSC-34 cells were differentiated with 1% serum and 1 μM RA. The probability of IK_{Ca}-channel openings occurring in undifferentiated cells was significantly higher than that in differentiated cells (Fig. 6A). For example, when an examined cell was maintained at −20 mV relative to the bath, IK_{Ca}-channel activity in undifferentiated cells was 0.013 ± 0.004 (n = 8); however, the channel open probability in undifferentiated cells was 0.005 ± 0.001 (n = 8, $P < 0.05$), which was significantly lower than the corresponding value in differentiated cells. Nevertheless, no clear difference in the amplitude of single IK_{Ca} channels between the two groups of cells was observed.

The *I-V* relationship of IK_{Ca} channels was further investigated and compared between undifferentiated and differentiated cells. As depicted in Fig. 6B, the single-channel slope conductance of IK_{Ca} channels obtained from various membrane potentials did not differ significantly between undifferentiated and differentiated cells (34 ± 1 pS [undifferentiated, n = 8] vs. 33 ± 1 pS [differentiated, n = 8], $P > 0.05$).

The effect of TRAM-34 on the activity of IK_{Ca} channels at various membrane potentials was further evaluated in undifferentiated NSC-34 cells. The voltage-dependent relation was determined using the Woodhull equation described in Materials and Methods. The values of K_0 and δ required to determine the inhibitory effect of TRAM-34 (1 μM) on IK_{Ca} channels in

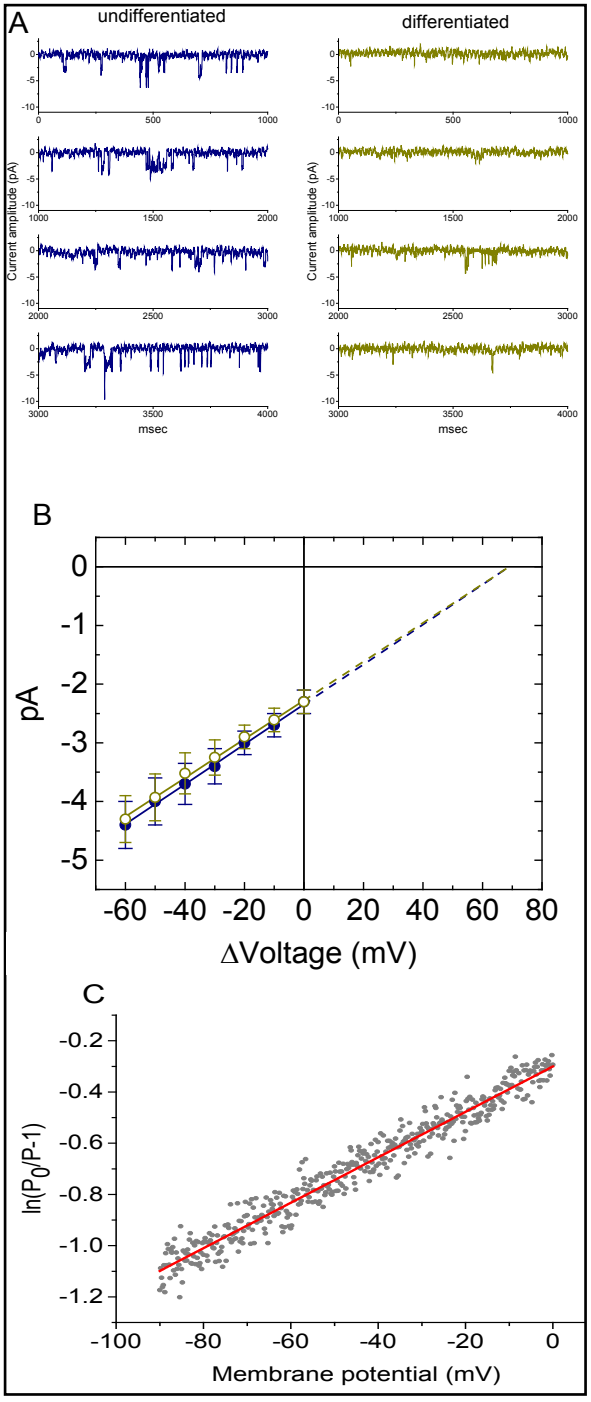

Fig. 6. Electrical properties of IK_{Ca} channels in undifferentiated and differentiated NSC-34 cells. To induce differentiation, cells were maintained in a culture medium with low serum (1%) and 1 μM RA. In these cell-attached current recordings, cells were bathed in normal Tyrode's solution containing 1.8 mM $CaCl_2$. (A) Representative IK_{Ca}-channel current traces in undifferentiated (left) and differentiated (right) NSC-34 cells. Each examined cell was maintained at −20 mV relative to the bath. Downward deflection indicates the opening event of the channel. (B) I-V relationships of single IK_{Ca}-channel currents in undifferentiated and differentiated cells (mean ± SEM; n = 8–11 for each point). The dashed line is pointing toward the value of reversal potential (i.e., 69 mV). Notably, because the patch potential is the sum of the resting potential plus the pipette potential, these inward currents reverse at approximately 69 mV. As the straight line is overlaid, the slopes of these two groups of cells become virtually indistinguishable. Single-channel amplitude was constructed and plotted as a function of potential (i.e., Δvoltage). (C) Voltage dependence for TRAM-34-mediated suppression of IK_{Ca} channels in undifferentiated NSC-34 cells. The activation curves with or without TRAM-34 (1 μM) were taken as the ramp pulse and was repeatedly increased from −90 to 0 mV within 1 s each time. The probabilities of IK_{Ca}-channel openings at different membrane potentials were obtained. The line overlaid onto the data was fitted using the Woodhull equation, as detailed in Materials and Methods. The values of K_0 (i.e., the equilibrium constant at 0 mV) and δ (i.e., the fraction of the membrane potential sensed by TRAM-34 (1 μM) at its binding site within the channel) required to determine the inhibitory effect of TRAM-34 on IK_{Ca}-channel activity were estimated to be 1.35 μM and 0.22, respectively.

undifferentiated cells were calculated to be 1.35 μM and 0.22, respectively (Fig. 6C). Based on these results, we deduced that the inhibitory effect of TRAM-34 on the probability of IK_{Ca}-channel openings occurring in undifferentiated NSC-34 cells is dependent on the TRAM-34 concentration and any changes in membrane potential.

Difference in mean closed time of IK_{Ca} channels between undifferentiated and differentiated NSC-34 cells

After observing that the closed-time duration of IK_{Ca} channels in NSC-34 cells tended to be prolonged after the cells had been induced to the differentiated state, we further examined and analyzed the kinetic properties of IK_{Ca} channels obtained with or without the induction of differentiation. As depicted in Fig. 7, the distribution of closed durations in undifferentiated and differentiated cells was fitted by a two-exponential function. When cells were differentiated with RA, the slow component of the mean closed time of these channels was significantly prolonged to 84 ± 5 msec from the control length (i.e., undifferentiated cells) of 69 ± 3 msec (n = 9, $P < 0.05$); by contrast, the fast component of the mean closed time did not differ between the two groups of cells (3.5 ± 0.1 msec [undifferentiated, n = 9] vs. 3.3 ± 0.1 msec [differentiated, n = 9], $P > 0.05$). Moreover, the mean open time of IK_{Ca} channels did not differ significantly between undifferentiated and differentiated cells (2.82 ± 0.03 msec [undifferentiated, n = 8] vs. 2.81 ± 0.04 msec [differentiated, n = 8], $P > 0.05$). These data clearly show that although no change in single-channel conductance occurred, cell differentiation with RA could significantly prolong the slow component of the mean closed time for IK_{Ca} channels in NSC-34 cells. Thus, differentiation-induced changes in IK_{Ca}-channel activity may have predominantly been a result of the increase in the duration of the slow component of the closed state.

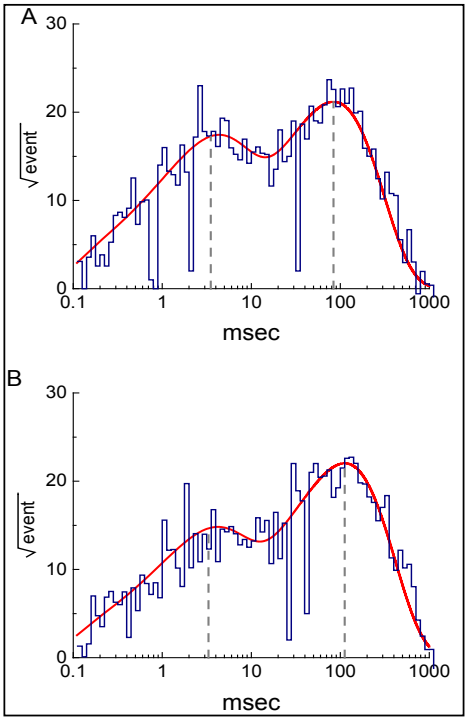

Fig. 7. Closed-time histogram of IK_{Ca} channels recorded from undifferentiated (A) and differentiated (B) NSC-34 cells. In these experiments, cells were bathed in normal Tyrode's solution, and the activity of IK_{Ca} channels was measured in a cell-attached configuration. In undifferentiated cells, data were obtained from measurements of 181 channel closings, with a total recording time of 2 min, whereas in differentiated cells, data were obtained from 145 channel closings, with a total recording time of 3 min. Notably, the abscissa and ordinate indicate the logarithm of closed time (msec) and the square root of the event number ($\sqrt{event}$), respectively. The smooth red line shown in each lifetime distribution was fitted using a two-exponential function, and the vertical dashed gray lines show the values of the time constant (i.e., fast and slow components). Notably, as cells were differentiated with low serum and RA, a shortening in the slow component of the mean closed time in the channel was observed; by contrast, no discernible change in the mean open time of the channel was noted.

IK_{Ca}-channel activity measured under inside-out current recordings in NSC-34 cells

The activity of IK_{Ca} channels obtained under cell-attached recordings could be regulated to any changes at the intracellular Ca^{2+} level. Another set of experiments based on inside-out recordings was conducted to investigate channel activity in undifferentiated and differentiated NSC-34 cells. As shown in Fig. 8, the examined cells were bathed in a high-concentration of K^+ solution containing 0.1 μM Ca^{2+}, and the membrane potential was maintained at −60 mV. IK_{Ca}-channel activity was readily detected in undifferentiated cells. When the bath medium was raised to 1 μM, the probability of IK_{Ca}-channel openings significantly increased. In sustained presence of 1 μM Ca^{2+}, further addition of TRAM-34 (1 μM) reduced the number of IK_{Ca} channels that would have otherwise been open, as evidenced by a significant reduction in the channel-opening probability to 0.013 ± 0.005 from the control level of 0.021 ± 0.002 (n = 8). Moreover,

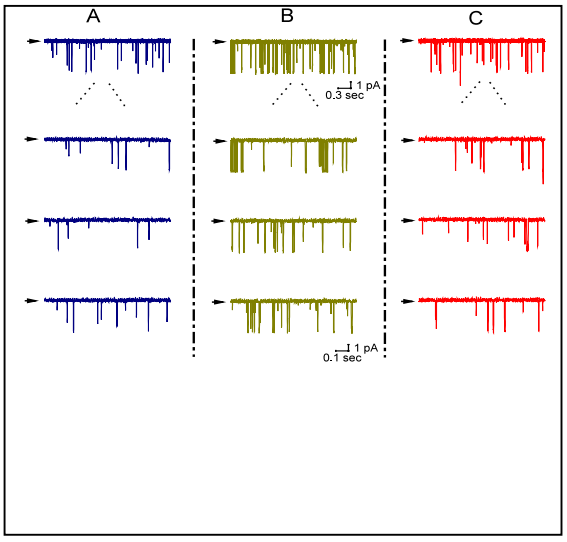

Fig. 8. IK_{Ca}-channel activity recorded under inside-out current recording. In these experiments, undifferentiated NSC-34 cells were bathed in a high-concentration of K^+ solution containing 0.1 μM Ca^{2+}, and the holding potential was set at −60 mV. Representative traces of IK_{Ca} channels in (A) and (B) were obtained as the detached patch was exposed to high K^+ solution containing 0.1 and 1 μM Ca^{2+}, respectively. In (C), when the patch was exposed to high K^+ solution containing 1 μM Ca^{2+}, TRAM-34 (1 μM) was further added to the bath (i.e., in the intracellular leaflet of the channel). The downward deflections are the opening events of the channel, and the arrowhead in each panel indicates the zero current level. The upper part of each panel corresponds to what appears in the lower part at an expanded scale.

channel activity in differentiated cells (0.011 ± 0.006, n = 7) was significantly lower than that in undifferentiated cells (0.021 ± 0.002, n = 8, $P < 0.05$).

Discussion

Consistent with previous observations [19, 20], our experimental results revealed that after RA treatment, NSC-34 cells could differentiate into motor neuron-like cells, as evidenced by the increased immune reactivity of neuronal differentiation in immunocytochemical studies. However, the RNA expression of $K_{Ca}3.1$ decreased during the differentiation process of NSC-34 cells. As such, a key speculation is that a reduction in K^+ permeability through IK_{Ca} channels is intimately associated with the differentiation of NSC-34 cells with RA.

In this study, we found that the density of depolarization-elicited $I_{K(DR)}$ in RA-differentiated NSC-34 cells was higher than that in undifferentiated NSC-34 cells, where I_K, which was subject to blockage by TRAM-34 (i.e., TRAM-34-sensitive I_K) but not by iberiotoxin or apamin, was also detected. TRAM-34 at a concentration of up to 5 μM exerted no significant effect on the proliferation of NSC-34 cells. However, the observed magnitude of TRAM-34-sensitive I_K in undifferentiated cells was considerably higher than that in RA-differentiated cells. Thus, as NSC-34 cells continue to differentiate with RA, the resultant decrease in the amplitude of TRAM-34-sensitive I_K due to the decreased activity of IK_{Ca} channels may not only produce a progressive reduction of K^+ efflux and depolarize the cell but also may result in the suppression of after-hyperpolarizing potentials [11, 14]. Such maintained membrane depolarization accompanied by an increase in neuronal excitability would be prepared to elicit voltage-gated Na^+ or Ca^{2+} currents in response to depolarizing inputs, thereby inducing regenerative neuronal firing [13, 26]. Thus, under cell-attached or inside-out recordings, a sustained decrease in IK_{Ca}-channel activity during RA-induced differentiation may ultimately be related to neuronal differentiation or excitability in NSC-34 cells.

Notably, the biophysical properties of IK_{Ca}-channel activity demonstrated slightly inward rectification or independence of voltage. However, the TRAM-34-sensitive current in undifferentiated NSC-34 cells was outwardly rectifying. Although the cause of this discrepancy is unknown, the presence of TRAM-34 may suppress other types of voltage-gated K^+ outward current expressed in NSC-34 cells.

The single-channel conductance of IK_{Ca} channels detected in NSC-34 cells was calculated as 34 pS, which is approximate to prototypical IK_{Ca} channels observed in other types of cells [2-5, 22, 25, 26] but distinguishable from that of large- and small-conductance Ca^{2+}-activated K^+ channels. The activity of these channels in NSC-34 cells was stimulated by DCEBIO and

9-phenenthrol but suppressed by TRAM-34; by contrast, diazoxide and verruculogen failed to influence channel activity. Moreover, in differentiated cells, the probability of IK_{Ca}-channel openings was lower, despite the lack of evident modification of single-channel conductance in the channel.

Based on our whole-cell and single-channel measurements, estimating the approximate density of IK_{Ca} channels recorded from undifferentiated NSC-34 neuronal cells may be possible. The whole-cell conductance of IK_{Ca} channels in an NSC-34 cell, *G*, is expressed as the equation $N \times \overline{P_O} \times \gamma$, where *N* is the number of channels, $\overline{P_O}$ is the average probability of channel openings, and γ indicates single-channel conductance. Figures 4 and 6 depict whole-cell and single-channel measurements taken at a $[K^+]_O$ of 5.4 mM, respectively where *G* was 13.3 nS and γ was 34 pS. Based on the measurements in single IK_{Ca}-channel kinetics, the value of $\overline{P_O}$ was estimated to be 0.011. Therefore, *N* was of the order of 34×10^3 channels/cells. The area of an undifferentiated cell was a 12×10^3 μm^2 based on cell size. Consequently, the densities of IK_{Ca}-channel openings that occurred in undifferentiated and differentiated cells were calculated to be approximately one channel per 0.345 μm^2 and one channel per 0.912 μm^2, respectively.

Because the single-channel conductance of IK_{Ca} channels was not modified in the presence of TRAM-34 or TRAM-39, the binding site lies mainly outside the transmembrane field. However, based on the Woodhull equation, the δ value (i.e., the proportion of the membrane voltage sensed at the binding site) required for TRAM-34-mediated inhibition of IK_{Ca} channels was estimated to be 0.22, suggesting voltage dependency in the suppression of activity in these channels. Therefore, sensitivity to TRAM-34 or other structurally similar compounds in NSC-34 cells or neurons occurring *in vivo* is conceivably dependent on the pre-existing level of resting potential, firing of action potentials, or concentration achieved by the compound in question.

The slow component of the mean closed time of IK_{Ca} channels was considerably prolonged as the cells were differentiated, whereas no significant difference in the fast component of the mean closed time or mean open time in the channel between undifferentiated and differentiated cells was observed. Thus, the transition from resting to open state is expected to be prolonged when cells are differentiated using RA. During the differentiation process, IK_{Ca} channels may have higher affinity for resting state than for open state.

During the process of differentiation using RA, the densities of $I_{K(DR)}$ in NSC-34 cells increased. Moreover, consistent with the observations of reductions in the amount of $K_{Ca}3.1$ mRNA and the immunofluorescent intensity of $K_{Ca}3.1$, the extent of TRAM-34-induced suppression of the I_K amplitude in response to a ramp pulse was significantly higher in undifferentiated cells.

In this study, cell differentiation reduced the functional expression of IK_{Ca} channels. Thus, the magnitude of the $K_{Ca}3.1$ current may be influenced by the electrical behaviors of neurons. However, studies have shown that the activity of IK_{Ca} channels can be enhanced under conditions where Ca^{2+} channels are facilitated by neuronal activity [9, 11, 13, 26]. Thus, notably, under culture conditions with no optimized stimulus, the activity of IK_{Ca} channels inherent in neurons occurring *in vitro* accompanied by any associated biochemical changes or signaling transduction processes could, to some extent, have been underestimated in the present study. The modulators of IK_{Ca} channels presented in this paper could be beneficial for the recovery of motor neurons during spinal cord injuries [12, 26, 27].

Abbreviations

DCEBIO (5, 6-dichloro-1-ethyl-1, 3-dihydro-2H-benzimidazol-2-one); DMEM (Dulbecco's modified Eagle's medium); FBS (fetal bovine serum); I_K *(*K^+ current*);* IK_{Ca} (channel, intermediate-conductance Ca^{2+}-activated K^+ channel); $I_{K(DR)}$, delayed-rectifier *(*K^+ current*); I-V (*current versus voltage*);* PBS (phosphate-buffered saline); RA (all-*trans*-retinoic acid); RT-PCR (reverse transcriptase–polymerase chain reaction); TRAM-34 (1-((2-chlorophenyl) (diphenyl)methyl)-1H-pyrazole); TRAM-39 (2-chloro-α,α-diphenylbenzeneacetonitrile); SEM (standard error of the mean).

Acknowledgements

The research that led to the composition of this manuscript was partially funded by grants from National Cheng Kung University (D106-35A13 and NCKUH-10709001) and Tainan City, Taiwan, through a contract awarded to S.-N. W. This research was supported in part by received funding from the Headquarters of University Advancement at the National Cheng Kung University, which is sponsored by the Ministry of Education, Taiwan, ROC. The authors are grateful to Ming-Chun Hsu and Yu-Kai Liao for earlier experiments and to Dr. Ke-Li Tsai at the Department of Physiology, Kaohsiung Medical University, Kaohsiung City, Taiwan, for technical assistance in this research. This manuscript was edited by Wallace Academic Editing.

Disclosure Statement

The authors declare no potential conflicts of interest or financial interests.

References

1 Liu SI, Chi CW, Lui WY, Mok KT, Wu CW, Wu SN: Correlation of hepatocyte growth factor-induced proliferation and calcium-activated potassium current in human gastric cancer cells. Biochim Biophys Acta 1998;1368:256-266.
2 Wu SN, Yu HS, Jan CR, Li HF, Yu CL: Inhibitory effects of berberine on voltage- and calcium-activated potassium currents in human myeloma cells. Life Sci 1998;62:2283-2294.
3 Fioretti B, Castigli E, Micheli MR, Bova R, Sciaccaluga M, Harper A, Franciolini F, Catacuzzeno L: Expression and modulation of the intermediate- conductance Ca2+-activated K+ channel in glioblastoma GL-15 cells. Cell Physiol Biochem 2006;18:47-56.
4 Shen AY, Tsai JH, Teng HC, Huang MH, Wu SN: Inhibition of intermediate-conductance Ca2+-activated K+ channel and cytoprotective properties of 4-piperidinomethyl-2-isopropyl-5-methylphenol. J Pharm Pharmacol 2007;59:679-685.
5 Huang MH, Huang YM, Wu SN: The Inhibition by Oxaliplatin, a Platinum-Based Anti-Neoplastic Agent, of the Activity of Intermediate-Conductance Ca(2)(+)-Activated K(+) Channels in Human Glioma Cells. Cell Physiol Biochem 2015;37:1390-1406.
6 Ju CH, Wang XP, Gao CY, Zhang SX, Ma XH, Liu C: Blockade of KCa3.1 Attenuates Left Ventricular Remodeling after Experimental Myocardial Infarction. Cell Physiol Biochem 2015;36:1305-1315.
7 Ishii TM, Silvia C, Hirschberg B, Bond CT, Adelman JP, Maylie J: A human intermediate conductance calcium-activated potassium channel. Proc Natl Acad Sci U S A 1997;94:11651-11656.
8 Nguyen TV, Matsuyama H, Baell J, Hunne B, Fowler CJ, Smith JE, Nurgali K, Furness JB: Effects of compounds that influence IK (KCNN4) channels on afterhyperpolarizing potentials, and determination of IK channel sequence, in guinea pig enteric neurons. J Neurophysiol 2007;97:2024-2031.

9 Bouhy D, Ghasemlou N, Lively S, Redensek A, Rathore KI, Schlichter LC, David S: Inhibition of the Ca(2)(+)-dependent K(+) channel, KCNN4/KCa3.1, improves tissue protection and locomotor recovery after spinal cord injury. J Neurosci 2011;31:16298-16308.
10 Lambertsen KL, Gramsbergen JB, Sivasaravanaparan M, Ditzel N, Sevelsted-Moller LM, Olivan-Viguera A, Rabjerg M, Wulff H, Kohler R: Genetic KCa3.1-deficiency produces locomotor hyperactivity and alterations in cerebral monoamine levels. PLoS One 2012;7:e47744.
11 King B, Rizwan AP, Asmara H, Heath NC, Engbers JD, Dykstra S, Bartoletti TM, Hameed S, Zamponi GW, Turner RW: IKCa channels are a critical determinant of the slow AHP in CA1 pyramidal neurons. Cell Rep 2015;11:175-182.
12 Turner RW, Kruskic M, Teves M, Scheidl-Yee T, Hameed S, Zamponi GW: Neuronal expression of the intermediate conductance calcium-activated potassium channel KCa3.1 in the mammalian central nervous system. Pflugers Arch 2015;467:311-328.
13 Lu R, Flauaus C, Kennel L, Petersen J, Drees O, Kallenborn-Gerhardt W, Ruth P, Lukowski R, Schmidtko A: KCa3.1 channels modulate the processing of noxious chemical stimuli in mice. Neuropharmacology 2017;125:386-395.
14 Cashman NR, Durham HD, Blusztajn JK, Oda K, Tabira T, Shaw IT, Dahrouge S, Antel JP: Neuroblastoma x spinal cord (NSC) hybrid cell lines resemble developing motor neurons. Dev Dyn 1992;194:209-221.
15 Ryu H, Jeon GS, Cashman NR, Kowall NW, Lee J: Differential expression of c-Ret in motor neurons versus non-neuronal cells is linked to the pathogenesis of ALS. Lab Invest 2011;91:342-352.
16 Wu SN, Hsu MC, Liao YK, Wu FT, Jong YJ, Lo YC: Evidence for inhibitory effects of flupirtine, a centrally acting analgesic, on delayed rectifier k(+) currents in motor neuron-like cells. Evid Based Complement Alternat Med 2012;2012:148403.
17 Hsu HT, Tseng YT, Lo YC, Wu SN: Ability of naringenin, a bioflavonoid, to activate M-type potassium current in motor neuron-like cells and to increase BKCa-channel activity in HEK293T cells transfected with alpha-hSlo subunit. BMC Neurosci 2014;15:135.
18 Hsu HT, Lo YC, Huang YM, Tseng YT, Wu SN: Important modifications by sugammadex, a modified gamma-cyclodextrin, of ion currents in differentiated NSC-34 neuronal cells. BMC Neurosci 2017;18:6.
19 Maier O, Bohm J, Dahm M, Bruck S, Beyer C, Johann S: Differentiated NSC-34 motoneuron-like cells as experimental model for cholinergic neurodegeneration. Neurochem Int 2013;62:1029-1038.
20 Ulrich H, Majumder P: Neurotransmitter receptor expression and activity during neuronal differentiation of embryonal carcinoma and stem cells: from basic research towards clinical applications. Cell Prolif 2006;39:281-300.
21 Wu SN, Yeh CC, Huang HC, So EC, Lo YC: Electrophysiological characterization of sodium-activated potassium channels in NG108-15 and NSC-34 motor neuron-like cells. Acta Physiol (Oxf) 2012;206:120-134.
22 Wu SN, Chen HZ, Chou YH, Huang YM, Lo YC: Inhibitory actions by ibandronate sodium, a nitrogen-containing bisphosphonate, on calcium-activated potassium channels in Madin-Darby canine kidney cells. Toxicol Rep 2015;2:1182-1193.
23 So EC, Huang YM, Hsing CH, Liao YK, Wu SN: Arecoline inhibits intermediate-conductance calcium-activated potassium channels in human glioblastoma cell lines. Eur J Pharmacol 2015;758:177-187.
24 Garland CJ, Smirnov SV, Bagher P, Lim CS, Huang CY, Mitchell R, Stanley C, Pinkney A, Dora KA: TRPM4 inhibitor 9-phenanthrol activates endothelial cell intermediate conductance calcium-activated potassium channels in rat isolated mesenteric artery. Br J Pharmacol 2015;172:1114-1123.
25 Yeh PS, Wu SJ, Hung TY, Huang YM, Hsu CW, Sze CI, Hsieh YJ, Huang CW, Wu SN: Evidence for the Inhibition by Temozolomide, an Imidazotetrazine Family Alkylator, of Intermediate-Conductance Ca2+-Activated K+ Channels in Glioma Cells. Cell Physiol Biochem 2016;38:1727-1742.
26 Sahu G, Asmara H, Zhang FX, Zamponi GW, Turner RW: Activity-Dependent Facilitation of CaV1.3 Calcium Channels Promotes KCa3.1 Activation in Hippocampal Neurons. J Neurosci 2017;37:11255-11270.
27 Hooten KG, Beers DR, Zhao W, Appel SH: Protective and Toxic Neuroinflammation in Amyotrophic Lateral Sclerosis. Neurotherapeutics 2015;12:364-375.